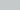



**Indian Ocean influence on the ENSO-Indian monsoon teleconnection is mostly apparent**

Tarun Bhatia & Anand S.  
ICS Centre for Climate Physics, Bhubaneswar, Odisha, India

### Apparent influence

Regarding the 'influence' of the Indian Ocean (IO) on the ENSO-Indian monsoon teleconnection, we intend to establish the 3-way relationship of the (1) ENSO, (2) IO, and (3) Indian monsoon. We represent the IO by the IIA,  $IA_{IO} = \frac{1}{N} \sum_{j=1}^N (IA_{IO}^j - \bar{IA}_{IO})$ , the ENSO by the IIA,  $IA_{ENSO} = \frac{1}{N} \sum_{j=1}^N (IA_{ENSO}^j - \bar{IA}_{ENSO})$ , and the IO by the IIA,  $IA_{IO} = \frac{1}{N} \sum_{j=1}^N (IA_{IO}^j - \bar{IA}_{IO})$ . The IO is the leading principal component (MJO) of the IO.

↓

### Apparent influence regionally

25. The correlation between the IO and the ENSO-Indian monsoon teleconnection is mostly apparent in the Indian Ocean region. The IO is the leading principal component (MJO) of the IO. The IO is the leading principal component (MJO) of the IO.

↓

### Influence cannot be detected in OBS

26. Furthermore, such an apparent regional influence is not detectable from the observational data. The IO is the leading principal component (MJO) of the IO. The IO is the leading principal component (MJO) of the IO.

↓

### Causality

27. The causal link between the IO and the ENSO-Indian monsoon teleconnection is mostly apparent in the Indian Ocean region. The IO is the leading principal component (MJO) of the IO. The IO is the leading principal component (MJO) of the IO.

↓

### Influence vs HO

28. However, in fact, the apparent influence of the IO on the ENSO-Indian monsoon teleconnection is mostly apparent in the Indian Ocean region. The IO is the leading principal component (MJO) of the IO. The IO is the leading principal component (MJO) of the IO.

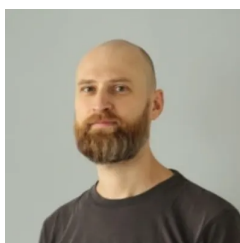
↓

### Influence vs HO

29. However, in fact, the apparent influence of the IO on the ENSO-Indian monsoon teleconnection is mostly apparent in the Indian Ocean region. The IO is the leading principal component (MJO) of the IO. The IO is the leading principal component (MJO) of the IO.

↓

IBS Center for Climate Physics, Busan, South Korea



**AGU FALL MEETING**  
New Orleans, LA & Online Everywhere  
13–17 December 2021

Poster Gallery  
brought to you by  
**WILEY**

# APPARENT INFLUENCE

Regarding the "influence of the Indian Ocean (IO) on the ENSO-Indian summer monsoon (ISM) teleconnection", we need to consider the 3-way relationship of the IO-ENSO-ISM. We represent the IO by the JJA-mean Indian Ocean Dipole index

([https://psl.noaa.gov/gcos\\_wgsp/Timeseries/DMI/](https://psl.noaa.gov/gcos_wgsp/Timeseries/DMI/)), IOD ( $I$ ), ENSO by the JJA-mean Nino3.4 ([https://psl.noaa.gov/gcos\\_wgsp/Timeseries/Nino34/](https://psl.noaa.gov/gcos_wgsp/Timeseries/Nino34/)) index ( $N$ ), and the ISM by the JJAS mean All-India summer monsoon rain index, AISMR ([https://tropmet.res.in/static\\_pages.php?page\\_id=53](https://tropmet.res.in/static_pages.php?page_id=53)) ( $A$ ), or, the local/regional summer monsoon rain ( $M(x)$ ).

1. Decorrelating IOD from Nino3.4,

$$I^* = I - \beta_1 N, \quad (1)$$

we have a significant (using the 20th c. CESM2-LE data [Rodgers et al. 2021] (<https://esd.copernicus.org/preprints/esd-2021-50/>) of 1e4 annual data points) but small *climatological* correlation coefficient  $r(I^*, A) = 0.06$  — actually dwarfed by the order of magnitude larger (in modulus)  $r(N, A) = -0.64$ . Here,  $\beta_1$  is the linear regression coefficient retaining  $i = 1$  in the nonlinear regression model

$$\Psi = \sum_{i,j=0}^3 \beta_{i,j} \Phi^i X^j + \sigma_\xi \xi, \quad (2)$$

while  $j = 0, \beta_0 = 0, \Phi = N, \Psi = I$ .

2. Therefore, we can hardly speak about “multiple determination” in terms of a linear regression model, as the *coefficient of multiple determination* or correlation is  $\sim r(N, A)$ .

3. In terms of the **nonlinear** regression model (2) ( $\Psi = A, \Phi = N, X = I^*$ ), however, with e.g.  $\beta_{1,1} \neq 0$  we could, possibly, still speak about multiple determination, or, an “**influence**” of the factor  $X = I^*$  on the ENSO-ISM teleconnection, as is customarily termed; or, if  $\beta_{1,1} = 0$ , then heteroscedasticity, i.e.,  $\sigma_\xi = \sigma_\xi(X)$  in (2), can still imply influence.

4. However, no heteroscedasticity is detected, and,  $\beta_{1,1}$  is insignificant.

5. Yet,  $\beta_{2,1} < 0$  is significant, which, together with the skewness  $\mu_3(N) > 0$ , would imply a slope  $S_{a,I^*} = da(N, A|I^*)/dI^*|_{(I^*=0)} < 0$ , in which we have the climatological **conditional** regression coefficient  $a(N, A|I^*)$  expressing an *apparent*  $I^*$ -influence.

6. However,  $S_{r,I^*} = 0.036 > 0$ . This should be due to  $S_{\sigma(N),I^*} < 0$ , considering a decomposition in terms of the textbook formula

$$r = a \frac{\sigma(\Phi)}{\sigma(\Psi)}. \quad (3)$$

7. Concerning the loosely corresponding “**apparent**” influence **as a correlation coefficient**  $R_{r,I^*} = r(r_\tau(N, A), \mu_\tau(I^*))$  of the “**apparent**”, i.e., **temporal**, mean  $I^*$ ,  $\mu_\tau(I^*)$ , on the **apparent** teleconnection,  $r_\tau(N, A)$ , we do have  $R_{r,I^*} > 0.192$  and  $R_{\sigma_\tau(N),I^*} = -0.43 < 0$ . But, considering (3), we also have a significant  $R_{\sigma_\tau(A),I^*} = -0.20 < 0$  opposing  $R_{\sigma_\tau(N),I^*}$ , whereas  $R_{a,I^*}$  is actually nonsignificant. That is, the apparnet influence is dominated by the apparent influence on ENSO variance/"amplitude".

## CAUSALITY

8. The lead-lag correlations, Fig. 1, reveal, however (contra point 7.), that concerning  $R_{\sigma_\tau(N),I^*}$ ,  $N$  is the dominant *causally influencing* process, whereas concerning  $R_{\sigma_\tau(A),I^*}$ ,  $I^*$  is in that role. Nevertheless, causality can go both ways (which can be supported by physical arguments); the lead-lag correlation is only to indicate **dominance**.

9. Still, we must conclude that **the Indian Ocean influence on the (apparent) ENSO-ISM teleconnection is mostly apparent**.

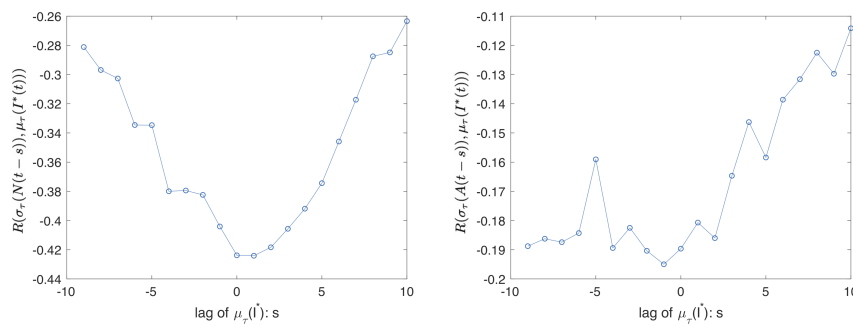


**Figure 1. Lead-lag correlations indicate causality in the CESM2-LE** data using all  $R = 100$  E-members in the period 1901-2000 of time span  $T = 100$  [yr]. With  $\tau = 20$  [yr], we would have 5 approximately independent  $r_\tau$ 's per E-member, that is,  $RT/\tau = 500$  data points in total. However, a maximal lead/lag of  $\tau/2 = 10$  [yr] is considered, which implies that in total, four instead of five 20th c. nonoverlapping  $\tau$ -blocks can be used.

## APPARENT INFLUENCE REGIONALLY

10. This conclusion carries over to ENSO teleconnections with local/regional monsoon precipitation  $M(x)$  in the ISM/AISMR domain, Fig. 2. Although, nontrivial patterns of  $R_{\sigma_T(M(x)),I^*}$  and  $R_{a_T(N,M(x)),I^*}$  give rise to a nontrivial pattern of  $R_{r_T(N,M(x)),I^*}$ .

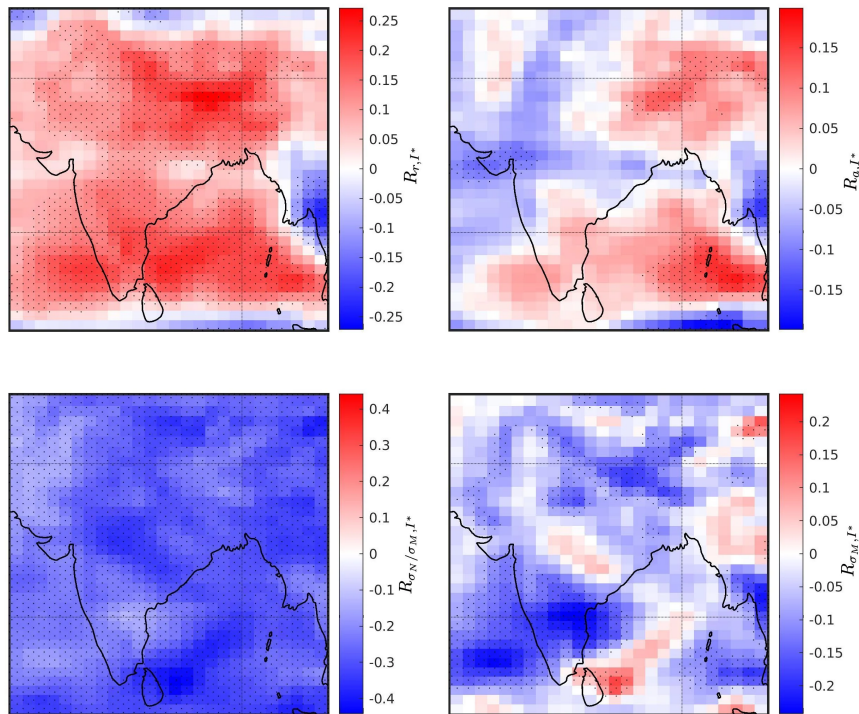


**Figure 2.** Decadal apparent influence of the Indian Ocean ( $I^*$ ) on the apparent ENSO-ISM teleconnection in view of a decomposition based on Eq. (3). (a)  $R_{r,I^*}$ , (b)  $R_{a,I^*}$ , (c)  $R_{\sigma_M,I^*}$ , and (d)  $R_{\sigma_N/\sigma_M,I^*}$ .



## INFLUENCE CANNOT BE DETECTED IN OBS

11. Furthermore, such an apparent regional influence is not detectable from 20th c. observational data concerning the variability of  $r_\tau$  (contra [Mahendra et al. 2021] (<https://rmets.onlinelibrary.wiley.com/doi/abs/10.1002/joc.6973>)) trying to reject  $H_0$ , Figs. 3, 4, 5. Yun & Timmermann (2018) (<https://agupubs.onlinelibrary.wiley.com/doi/full/10.1002/2017GL076912>) (YT18) already showed this with a box-average.

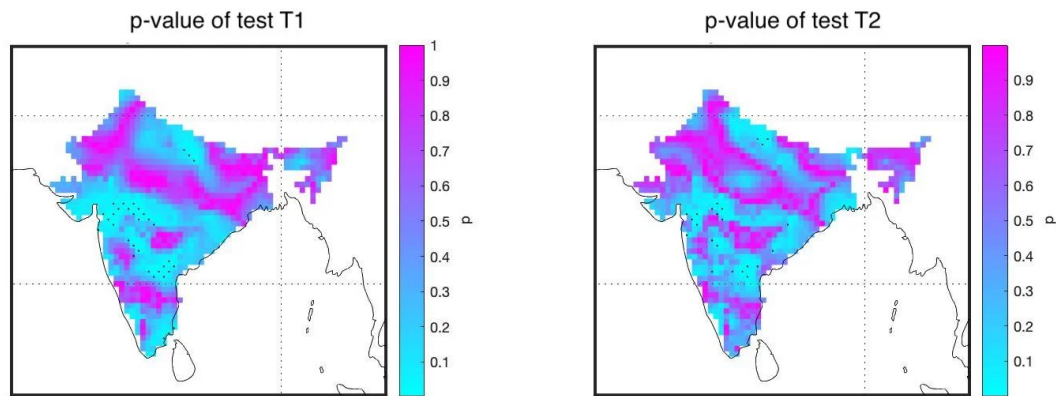


Figure 3. Testing for the null-hypothesis  $H_0$  that the ENSO-ISM relationship, represented by the correlation coefficient  $r(N, M(x))$  between JJA Nino3.4 and JJAS local gridpoint-wise precipitation, obeys a linear regression model [YT18], as described under point 1. (a) Test T1 uses the test statistic  $\text{std}[r_\tau]_{t=t_0}^{t_f}$ ,  $\tau = 20$  [yr], selecting an observational period within the intersection of those of the CRU PREv4.03 and ERSSTv5 data series:  $t_0 = 1901$ ,  $t_f = 2000$  [yr]. (b) T2 uses the test statistic of the maximal rapid change,  $\max\|r_{\tau^*}(t) - r_{\tau^*}(t + \tau^*)\|_{t=t_0}^{t_f}$ ,  $\tau^* = \tau = 20$  [yr]. See also Figs. 4, 5.

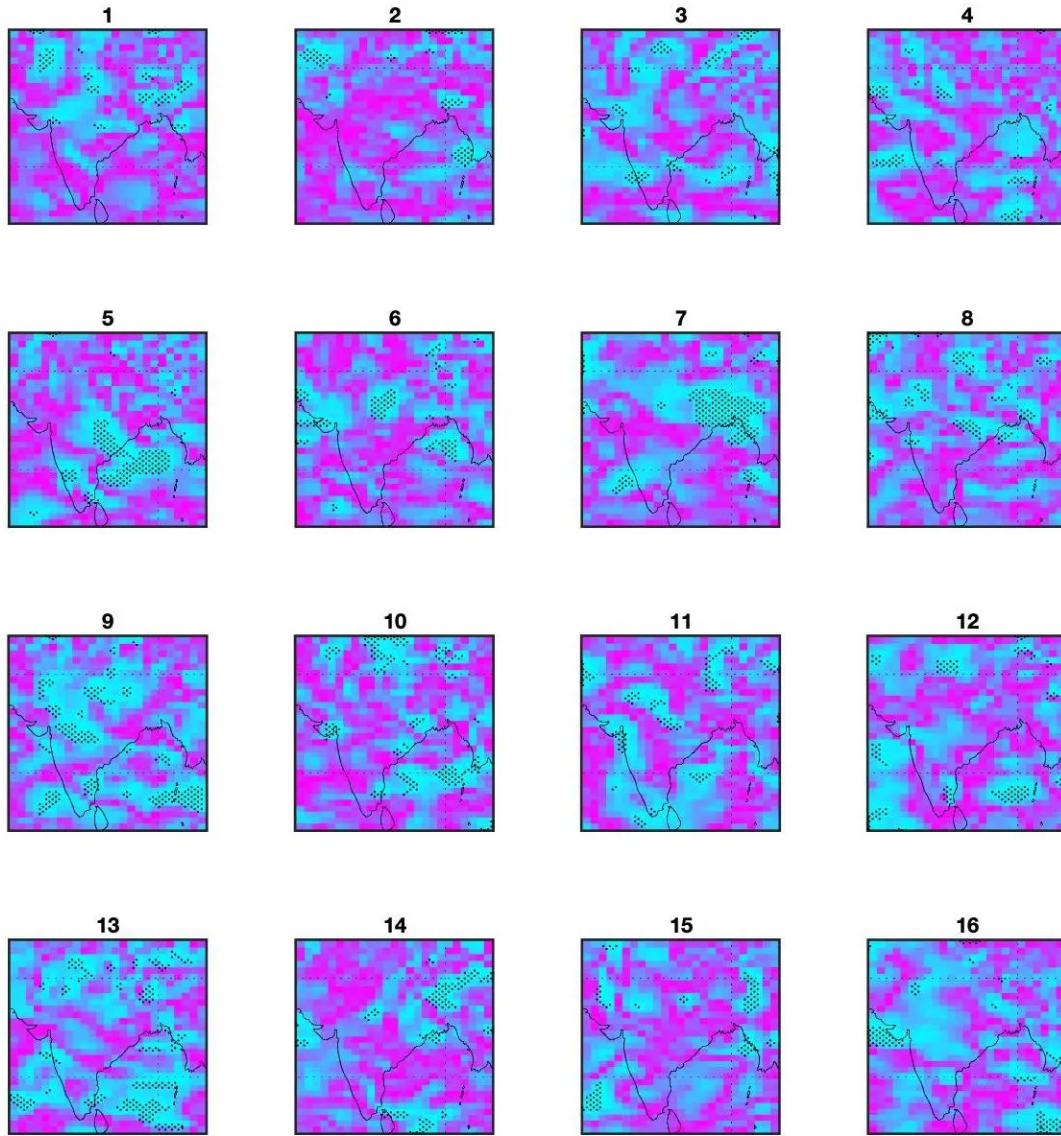


Figure 4. Stamp diagram of p-values of T1 analogous to those in Fig. 3a, but here, instead of observational data, we consider single realisations of the CESM2-LE per diagram. Stippling indicates significance ( $p < 0.05$ ). Areas of significance seem to be unrelated between different realisations, signaling their falseness. See also Fig. 5.

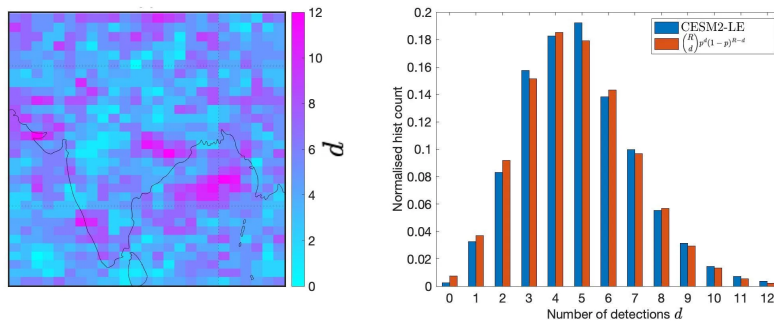
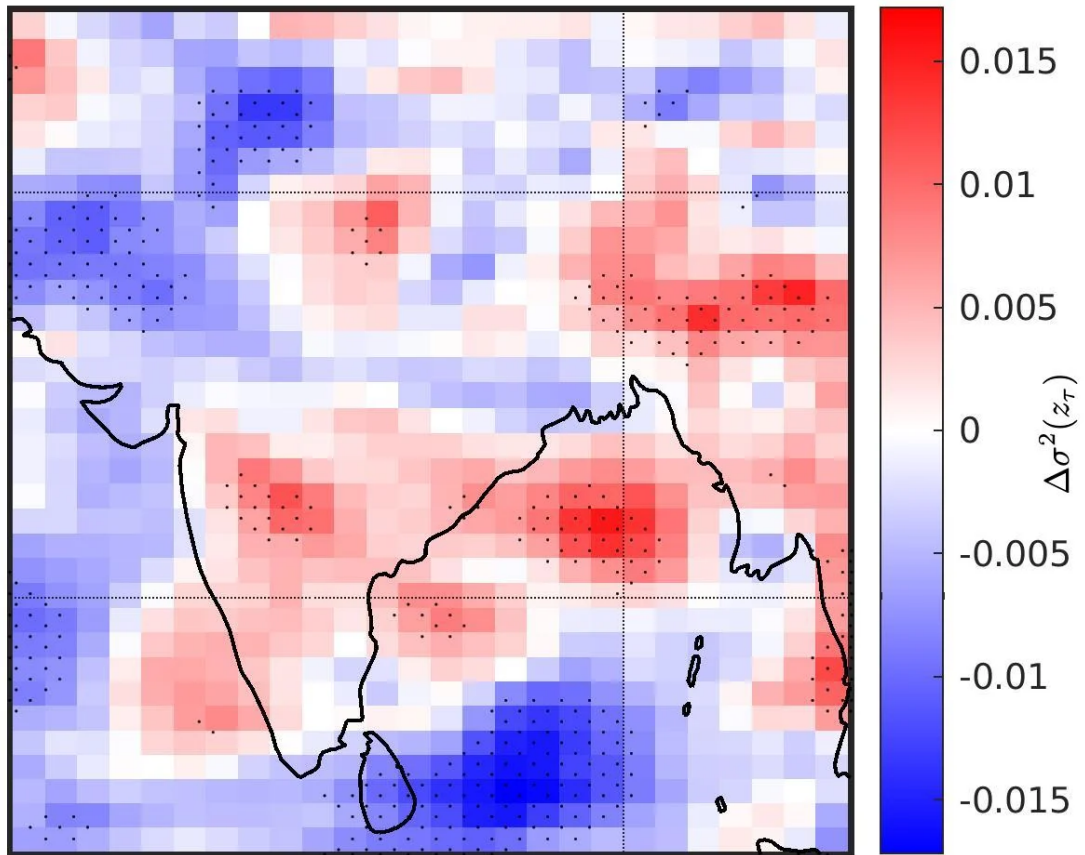


Figure 5. (a) Spatial distribution of detection counts  $d$  out of the  $R = 100$  realisations/members of the CESM2-LE (a subset of which is shown in Fig. 4). (b) Normalised distribution of detection counts wrt. gridpoints (seen in panel (a)), compared to the binomial distribution  $\binom{R}{d} p^d (1-p)^{R-d}$  made with  $p = 0.048$  for best match.

## INFLUENCE VS H0

12. However, in fact, the apparent influence  $R_{r,I^*}$  is not necessarily fully incompatible with  $H_0$  (contra YT18); see the mismatch of Fig. 6 with Fig. 2a. This should be why the apparent influence is more detectable than a departure from  $H_0$ .



**Figure 6. Testing  $H_0$  in the CESM2-LE** using all  $R = 100$  E-members in the period 1901-2000 of time span  $T = 100$  [yr]. The map shows the difference  $\Delta\sigma^2(z_\tau) = \sigma^2(z_\tau) - \sigma_0^2$  between the actual variance of the Fisher transformation of the moving window cc,  $z_\tau = \text{atanh}(r_\tau)$ , bw. Nino3.4 ( $N$ ) and the ISM ( $M(x)$ ) and what is predicted by  $H_0$ . With  $\tau = 20$  [yr], we have 5 approximately independent  $r_\tau$ 's per E-member, that is,  $RT/\tau = 500$  data points in total. The stippling marks significant values in terms of a one-sample F-test performed by Matlab's `varstest` for the equality of variances.

## ABSTRACT

Origins of the interdecadal fluctuations of the ENSO-Indian summer monsoon (ISM) teleconnection strength measured by running window correlation coefficients have been much debated. The main question is whether it's due mostly (i) to sampling errors, or, (ii) under internal variability decadal time scale drivers modulate it, and/or, (iii) it has undergone some forced change recently. A new statistical test does not detect any of (ii-iii) in observations. However, it does not mean that there could not be such effects, just that the data is insufficient. Large ensemble data sets are well suited to investigate these questions. Previously, (iii) was found to be small (even if possibly important) in the MPI-GE data set, and the situation is similar in the new CESM2-LE data set. This time we investigate (ii), too, and find that the decadal variability of e.g. the Dipole Mode Index (DMI) of the Indian Ocean explains 4% of the apparent variability of the ENSO-ISM teleconnection. If the CESM2-LE were faithful to reality, then this signal would take two millenia to have a 50% chance to detect. We also find that the DMI influence is due to the nonlinearity of the three-way ENSO-ISM-DMI relationship in the form of a regression model, not heteroscedasticity.

